The Electroreductive Dehalogenation Reaction of 5-Bromo-2-chlorobenzoic Acid on Dendritic Ag/Cu

Fen Wang[1], Zhong Quan Fan[1], Xiao Hua Wu[2], Mei Chao Li[1,*], Chun An Ma[1,*]

[1]College of Chemical Engineering, Research Center of Analysis and Measurement, Zhejiang University of Technology, Hangzhou 310032, China
[2]College of Chemistry and Life Science, Zhejiang Normal University, Jinhua 321004, China
[*]E-mail: limc@zjut.edu.cn (M.C. Li), science@zjut.edu.cn (C.A. Ma)

Dendritic Ag/Cu electrode was synthesized by galvanic replacement of $AgNO_3$ and Cu, and was investigated by scanning electron microscopy, transmission electron microscopy and X-ray diffraction. Cyclic voltammetry and in situ FTIR were combined to study the electroreductive dehalogenation reaction of 5-bromo-2-chlorobenzoic acid (BCBA) on Ag/Cu electrode in NaOH aqueous solution. Ag/Cu electrode exhibited high electrocatalytic activity for the dehalogenation reaction of BCBA. Based on the in situ FTIR data, the electroreductive dehalogenation process of BCBA was represented as a sequence of halide expulsions and hydrogen additions. Because the bond dissociation energy value of C-Br bond was less than that of C-Cl bond, Br^- was easier to release from benzene ring. With the C-Br breakage, BCBA received electrons and hydrogen to form intermediate 2-chlorobenzoate. Then C-Cl broke in the same way, and the end product benzoate was obtained.

1. INTRODUCTION

Halogenated aromatic compounds are widely used in pesticides and household products [1-3]. It is well known that most of halogenated aromatic compounds are toxic with the halogen contained in their structure, while halogen-free compounds are usually much less toxic. In addition, less harmful and more valuable compounds can be obtained by dehalogenation reaction with high product yield [4]. Therefore, dehalogenation reaction of halogenated aromatic compounds is important for its social benefit and economic returns. Traditional treatment processes such as biodegradation [1,2], metal reductive dehalogenation [5,6], photodegradation are not quite effective for the dehalogenation of

halogenated aromatic compounds [7]. Electroreductive dehalogenation technology is quite effective under mild experimental condition, and has been proved to be one of the most attractive methods [4,8].

The electrode material shows influence on the dehalogenation reaction during the degradation process. Silver (Ag) cathode possesses extraordinary electrocatalytic activity toward dehalogenation reduction, and the halide acts as a bridge R⋯X⋯Ag between the electrode surface and the reacting substrate [9,10]. Recently, dendritic Ag has attracted considerable interest due to their fascinating geometric properties, and agglomeration of Ag nanoparticles is difficult to happen during the preparing processes. Varying measures have been used to synthesis Ag dendritic nanostructures, such as galvanic displacement [11-14], electrochemical deposition [15] and wet-chemical method [16]. Up to now, most of the dendritic Ag is mainly applied in surface enhanced Raman scattering (SERS) [11-13,16], catalysis [14,17], and sensing [18]. According to the literature survey, electrocatalytic activity of dendritic Ag for electroreductive dehalogenation of halogenated aromatic compounds has never been reported. Cu and Ag/Cu nanoparticles process excellent electrical conductivity and exhibits high electrocatalytic activity to certain halogenated aromatic compounds during the electrochemical process [19-21]. The galvanic replacement reaction of $AgNO_3$ and Cu to get dendritic Ag/Cu is a very simple method without complicated equipments or special reductive reagents. Therefore, dendritic Ag/Cu is synthesized by galvanic displacement under room temperature and is used in the electroreductive dehalogenation reaction of halogenated aromatic compound in this paper.

In addition, the electronegativity of substituent groups and the position of halogen atoms in the benzene ring also show effect on the dehalogenation reaction [22,23]. Halogenated benzoic acid 5-bromo-2-chlorobenzoic (BCBA), which has two halogen atoms bromine and chlorine, is chosen as the template molecule in this paper. Its dehalogenation sequence and mechanism are studied using in situ FTIR, cyclic voltammetry and DFT calculation.

2. EXPERIMENTAL

2.1 Reagents

The following reagents were purchased from the indicated suppliers and used without further purification: 5-bromo-2-chlorobenzoic acid (BCBA, 98%), silver nitrate ($AgNO_3$, AR), sodium hydroxide (NaOH, 96%). All the solutions were prepared from ultrapure water supplied by a Milli-Q system (Millipore, Japan).

2.2 Preparation and characterization of Ag/Cu

The clean Cu substrate was immersed into the deposition solution of 5 mM $AgNO_3$ for 20 min, and Ag/Cu electrode was obtained by replacement reaction of $AgNO_3$ and Cu. Then Ag/Cu electrode was rinsed in ultrapure water and dried in air. In principle, the driving force for the galvanic replacement reaction is the electric potential difference between Ag^+ and Cu.

The metal micro/nanostructures were characterized by scanning electronic microscope (SEM, Hitachi S4700) at an accelerating voltage of 15 kV. Transmission electron microscopy (TEM), High-resolution transmission electron microscopy (HRTEM) and corresponding selected area electron diffraction (SAED) were preformed on a high resolution transmission electron microscope (TEM, FEI, Tecnai G2 F30 S-Twin)operated at 300 kV. X-ray diffraction (XRD) characterization was measured by an X-ray diffractometer (Thermo SCINTAG X00 TRA, Cu-Kα□ X-ray radiation, λ=0.15418 nm). For TEM observations, dendritic Ag was released from Cu substrate. The samples were prepared by ultrasonic dispersion in ethanol, then the suspension was dropped onto a conventional carbon-coated nickel grid and dried in air before analysis.

2.3 Cyclic voltammetry experiments

All voltammetric measurements were tested with a standard three-electrode cell using a model 263 Potentiostat/Galvanostat (EG&G, USA). Ag/Cu, Ag and Cu with the geometric area of 0.08 cm^2 were used as the working electrode. The platinum sheet (3.0 cm^2) and a saturated calomel electrode (SCE) were used as the counter electrode and the reference one, respectively. All potentials reported in this paper were relative to that of SCE.

2.4 In situ FTIR experiments

In situ FTIR spectra were obtained with a Nicolet 670 FTIR spectrometer equipped with a MCT-A detector cooled by liquid nitrogen. The spectroelectrochemical cell was of a standard three electrode type and coupled to a CaF$_2$ disk window (32 mm × 2 mm). The resulting spectrum was reported as the relative change in reflectivity that was calculated as:

$$\Delta R / R = [R(E_S) - R(E_R)] / R(E_R) \qquad (1)$$

where $R(E_S)$ and $R(E_R)$ were the single-beam spectra of reflection collected at sample potential E_S and reference potential E_R, respectively [24]. As a result, negative-going bands in the resulting spectra indicate the formation of intermediates or products in the thin layer solution during the reaction, while positive-going bands denote the consumption of reactants. Each spectrum corresponds to 200 interferometer scans at 8 cm^{-1} resolution. The reference potential was 0 V and the polarization time at each potential was about 90 s.

2.5 Electrolysis

The electrolysis experiments were performed in a two-compartment electrolytic cell separated by a cation-exchange membrane (Nafion 117), and assembled with magnetic stirring bar. The cathode was Ag/Cu cathode (2 cm×4 cm) and a graphite flake (2 cm×4 cm) was used as the anode. The electrolysis experiment was performed on laboratory direct current power in alkaline solution containing 5 mM BCBA with the constant current 150 mA. High performance liquid chromatography

(HPLC) with a Waters 2487 detector was used to measure the concentrations of the parent chlorinated compound and products.

2.5 Computations details

The calculations have been performed in the framework of DFT. DFT/B3LYP/6-311G++(d,p) was carried out to calculate geometry optimization, which is confirmed by FTIR frequency calculations and each of the geometries is minimum on the potential energy surface. The bond dissociation energy (BDE) values of C-Br and C-Cl have been calculated according to the expression [25]:

$$DH^0(R-X) = \Delta_f H^0(R\cdot) + \Delta_f H^0(X\cdot) - \Delta_f H^0(R-X) \quad (2)$$

In this case, $\triangle_f H^0$ represented the heats of formation of the respective species in the ideal gas state at 1 atm. All the calculations were performed with the Gaussian03 package program.

3. RESULTS AND DISCUSSION

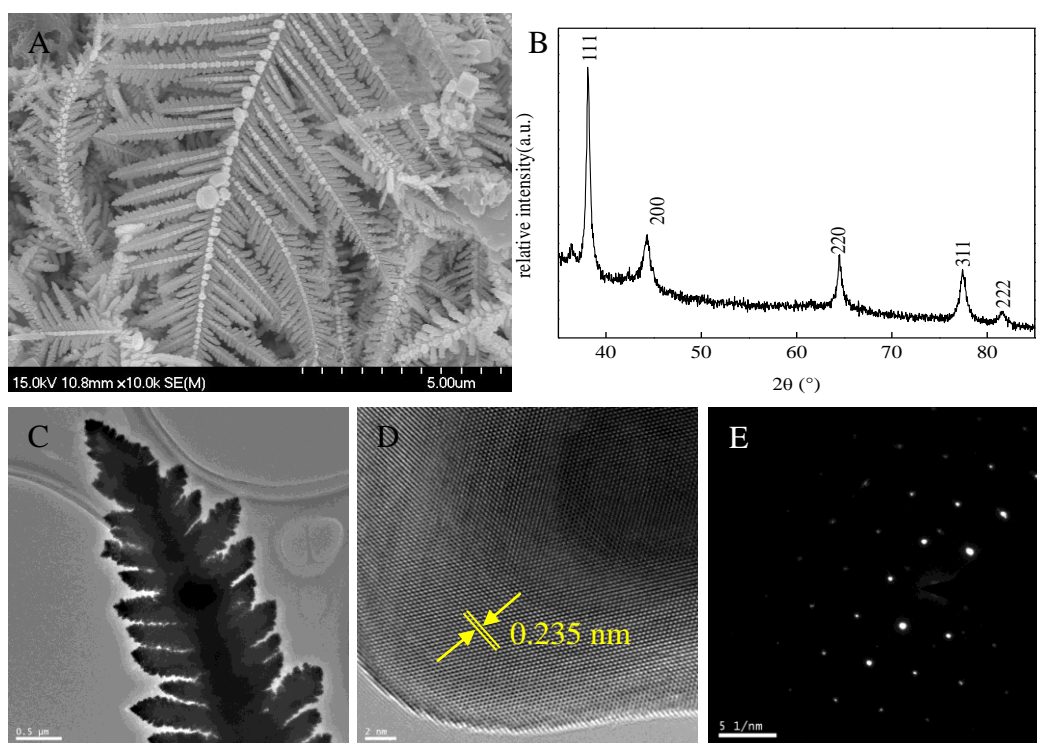### 3.1 Characterization of Ag/Cu electrode

Figure 1. (A) SEM image of the nano-Ag on the Cu substrate; (B) the XRD pattern; (C) TEM image of dendritic nano-Ag; (D)HRTEM image of the Ag branch tip; (E) the corresponding SAED pattern.

Fig. 1A displays the morphology of Ag on the Cu electrode. It showed that Ag was deposited on the Cu surface evenly without agglomeration. Most of the Ag particles exhibited typical and beautiful dendrites, which consisted of a long central backbone with many branches. A typical XRD pattern of Ag dendrites is present on Fig. 1B, indicating that the crystallinity of the dendrites was high. The five diffraction peaks could be indexed to diffraction from the (111), (200), (220), (311), and (222) of cubic silver (JCPDS Card File, 03-065-2871). Dendritic Ag structures are more obviously displayed in the TEM image (Fig. 1C). The lattice fringes spacing of nano-Ag was 2.35 Å (Fig. 1D). It was assigned to the interplanar spacing of (111), the most stable crystal plane of silver. This point was further proved by the selected area electron diffraction (SAED) pattern of Ag dendrite (Fig. 1E). Furthermore, the six-fold symmetry of the diffraction spots clearly revealed that the dendritic nano-Ag was a single crystal [14]. Based on the above analysis, it could get the conclusion that the growth direction of the dendritic nano-Ag was preferential in the (111) direction.

3.2 cyclic voltammetry studies

The electrocatalytic activity of Ag/Cu for electroreductive dehalogenation reaction of BCBA in NaOH solution was investigated by cyclic voltammetry, as plotted in Fig. 2(A). For the sake of clarity, cyclic voltammogram of Ag/Cu in the blank solution without BCBA was obtained too. The reduction current was well evidenced with onset potential at about -0.9 V on Ag/Cu electrode. With the potential negative going, the reduction current increased gradually and the peak current of 9.86 mA was observed at -1.30 V on Ag/Cu electrode, and the peak was related to the electroreduvtive reaction of BCBA on Ag/Cu electrode. It indicated that Ag/Cu showed good electrocatalytic activity to BCBA. There was no corresponding oxidation peak of BCBA in the positive going potential sweep. Thus, the electroreductive dehalogenation reaction of BCBA was irreversible [4, 31].

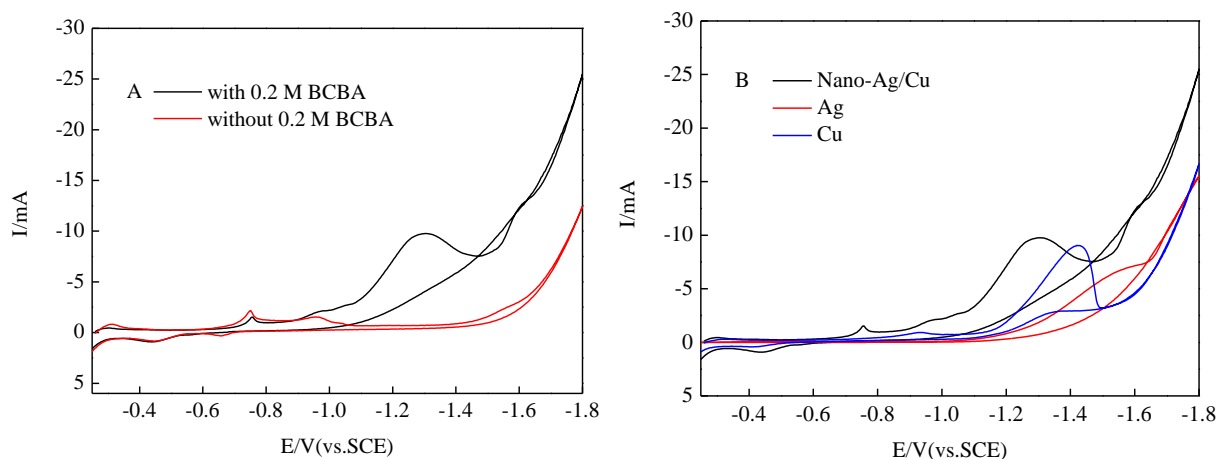Fig. 2(B) shows the electrochemical behavior of Ag/Cu in comparison with Cu an Ag under the similar solutions.

Figure 2. Cyclic voltammograms for the reduction of 0.2 M BCBA in 1 M NaOH. (A) on Ag, Cu and nano-Ag/Cu electrode; (B) with and without BCBA on nano-Ag/Cu electrode.

It could be observed that there was a weak reduction peak on Ag electrode at the potential more negative than -1.5 V, indicating that metal Ag possessed weak electrocatalytic properties toward the electroreductive dehalogenation reaction of BCBA. In addition, the peak current on Cu electrode was about 9.06 mA with the peak potential -1.42 V. But the peak potential of Ag/Cu electrode was more positive and the peak current was higher as compared with those of the Ag and Cu electrodes. Thus, Ag/Cu electrode possessed the relatively remarkable electrocatalytic activity for electroreductive dehalogenation reaction of BCBA as compared with Ag and Cu electrodes under the similar conditions.

3.3 In situ FTIR studies

In situ FTIR spectra of BCBA on Ag/Cu electrode were recorded during electroreductive dehalogenation process in the spectral range of 1600-1000 cm^{-1} are shown in Fig.3. When the sample potentials were more positive than -300 mV, no obvious changes could be observed on the FTIR spectra in Fig. 3. This result indicated that the electroreductive dehalogenation reaction of BCBA on Ag/Cu electrode was quite slow.
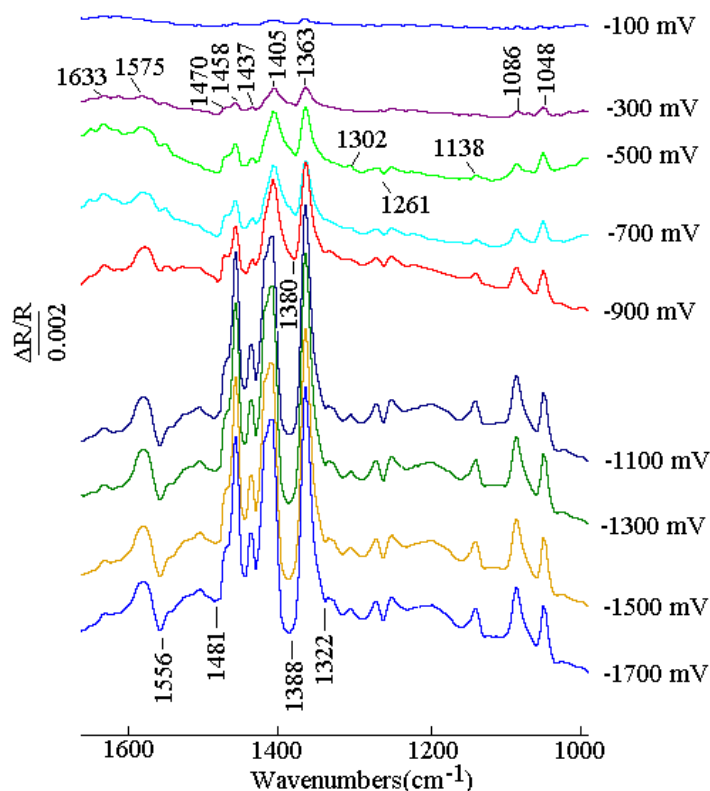

Figure 3. In situ FTIR spectra collected during electroreductive dehalogenation reaction of BCBA on nano-Ag/Cu electrode.

At -300 mV, the positive-going bands could be observed. Table 1 summarizes the assignments of all the band wavenumbers in the paper in detail. The positive-going bands located at 1470, 1458 and

1437 cm^{-1} were most likely associated with C-C ring stretching modes of BCBA [26, 27]. The bands at 1405 and 1363 cm^{-1} were due to symmetric stretching vibration of carboxyl (ν_s(COO)) of BCBA [28,29], The band 1575 cm^{-1} was related to C-C ring stretching and asymmetric vibration of carboxyl [27,28].

In addition, 1633 cm^{-1} might due to the bending vibration of water in the thin layer [30]. It was noteworthy that the important positive-going bands at 1086 and 1048 cm^{-1} were observed, which were assigned to C-Cl and C-Br stretching vibration of BCBA, respectively [31]. These positive-going bands were mainly due to the loss of BCBA in the thin layer solution between Ag/Cu disc electrode and CaF$_2$ window. The peak intensity of C-Br was stronger than that of C-Cl, indicating that C-Br was easier to break than C-Cl with the positive potential, and the debromination reaction was the main reaction. But it was difficult to be observed from cyclic voltammetry (Fig. 2).

In addition, negative-going bands were also observed at the same potential in Fig. 3. The bands at 1556 cm^{-1} was related to C-C ring stretching vibration and ν_s(COO) of 2-chlorobenzoate, 1380 and 1481 cm^{-1} were assigned to its ν_s(COO) and C-C ring stretching vibration of 2-chlorobenzoate [32]. When the potential stepped to more negative values, the electrochemical reaction get more and more fiercely on the electrode and all the peak intensities increased gradually. The other four bands 1322, 1302, 1138 and 1261 cm^{-1} assigned to BCBA and 2-chlorobenzoate could be obviously observed. The two positive-going bands at 1302 and 1138 cm^{-1} were associated with C-O stretching vibration and C-H in-plane bending vibration of BCBA [28,31], and the negative-going band 1322 and 1261 cm^{-1} was assigned to C-O stretching vibration of 2-chlorobenzoate. The negative-going band was indicative of the gain of the intermediate or product in solution of the thin layer. Based on above analysis, the main intermediate of electroreductive dehalogenation reaction of BCBA was 2-chlorobenzoate.

Table 1. The corresponding assignments of all the bands.

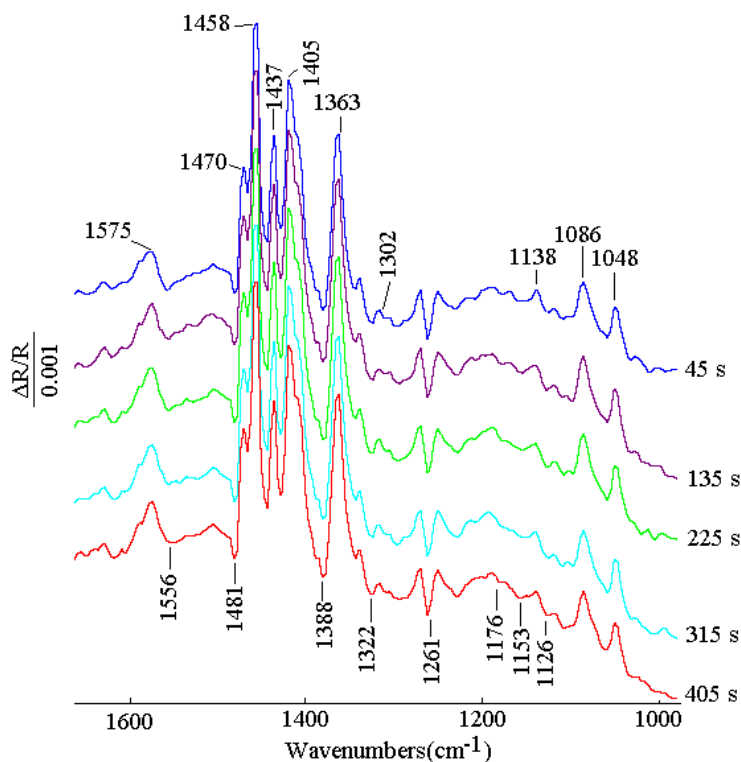| Band	Wavenumbers/cm^{-1}	Assignments
Positive-going	1470, 1458 and 1437	C-C ring stretching modes of BCBA
	1405 and 1363	ν_s(COO-) of BCBA
	1575	ν_{as}(COO-) and C-C ring stretching vibration of BCBA
	1086	C-Cl stretching vibration of BCBA
	1048	C-Br stretching vibration of BCBA
	1302	C-O stretching vibration of BCBA
	1138	C-H in-plane bending vibration of BCBA
	1633	bending vibration adsorbed water
negative-going	1556	ν_{as}(COO-) and C-C ring stretching vibration of 2-chlorobenzoate
	1380	ν_s(COO) of 2-chlorobenzoate
	1322, 1481	C-C stretching vibration of benzene ring
	1261	C-O stretching vibration of 2-chlorobenzoate
	1388	ν_s(COO) of benzoate
	1176, 1153, 1126	C-H bending vibration of benzoate

Figure 4. Time-resolved FTIR spectra collected during electroreductive dehalogenation reaction of BCBA on Ag/Cu electrode at -1700 mV.

At -1100 mV, the new bands at 1388 cm^{-1} was observed, which was assigned to ν_s(COO) of benzoate. In addition, the peak intensity of C-Cl band was higher than that of C-Br band, and C-Cl was easier to break. As the potential stepped to more negative, no new bands were observed.

In order to observe C-H in-plane bending of benzoate obviously and to verify the final product, time-resolved FTIR (TR-FTIR) spectra were collected during electroreduction process of BCBA on Ag/Cu electrode at -1700 mV. As shown in Fig. 4, the negative-going bands at 1176, 1153 and 1126 cm^{-1} were observed. The band at 1176 cm^{-1} was associated with C-H in-plane bending of benzoate [33], while the band at 1153 and 1126 cm^{-1} were generated from C-H formation after C-X (X=Br, Cl) breakage. Based on these results obtained and the literature [26], it could be verified that BCBA received an electron to form BCBA radical anion, which lost the Br anion. Then the intermediate 2-chlorobenzoate was got after the free radical received another electron and a proton at the positive potential and the reaction was weak, Cl anion released in the same way. The final product of electroreductive dehalogenation reaction of BCBA was benzoate.

3.4 Theoretical calculate

With the ongoing growth of computational technology, theoretical calculation became more convenient. J. Suegara et al proposed clearly that BDE values could predict the dechlorination pathway [34]. According to the expression (2), the BDE values of C-X (X=Cl, Br) were got. The geometric construction of BCBA molecule and the BDE values of C-X were shown in Fig. 5. COO and benzene ring was not in a plane due to the steric effect of Cl. As compared with C-Br bond, the BDE value was

higher and the bond length was shorter. It was well known that the lower the BDE value was, the easier for the bond to break. So C-Br bond of BCBA was easier to break than C-Cl bond, which coincided well with the results of in situ FTIR.
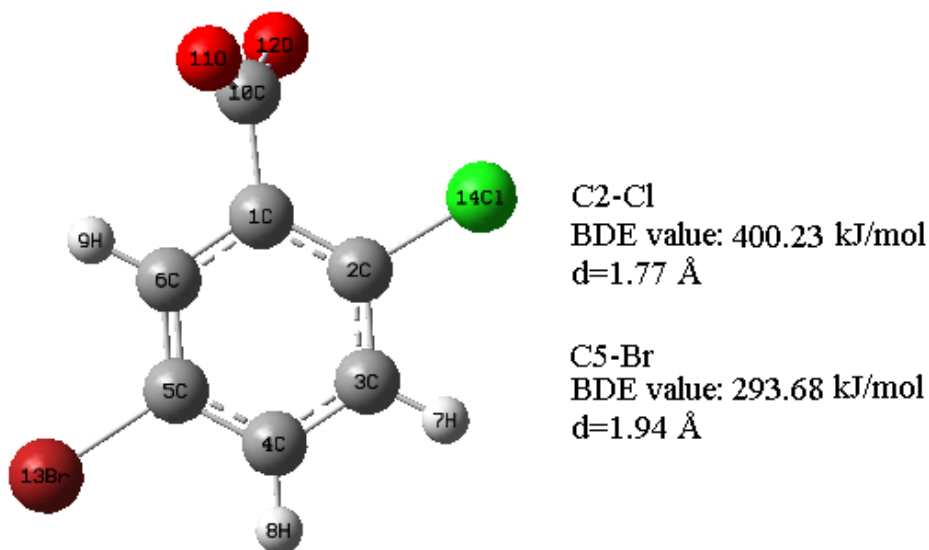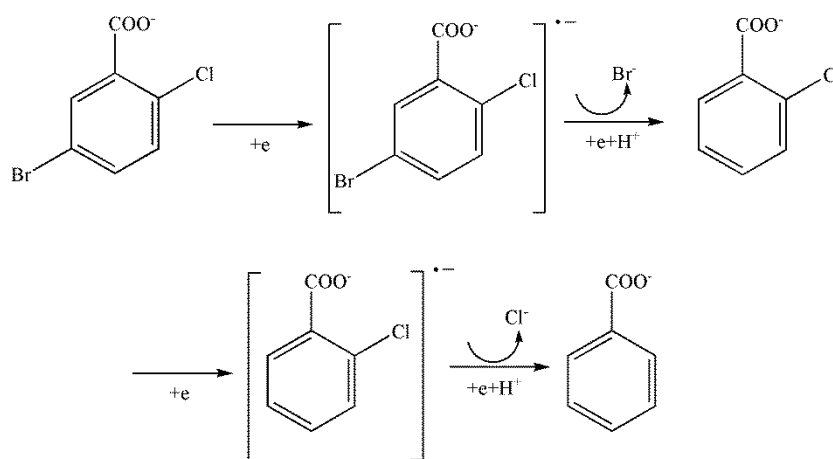

Figure 5. The BDE values and the length of C-X bonds of BCBA

High performance liquid chromatography (HPLC) was carried out to identify the content of the starting materials, intermediates and products. It was found that the intermediate product was 2-chlorobenzoate, and the end product was benzoate without other compounds. Taking into account the experiment results and the literatures [26,33], the mechanism of BCBA on Ag/Cu electrode was obtained and shown in Scheme 1. Firstly, BCBA received an electron to form BCBA radical anion, which lost a bromine ion in the C2 position and formed 2-chlorobenzoate free radical. Then the free radical received another electron and a proton to give the intermediate 2-chlorobenzoate. Finally, Cl anion in the C2 position released in the same way and generated the final product benzoate.

Scheme 1. Mechanism of electroreductive reaction of BCBA on Ag/Cu electrode.

4. CONCLUSIONS

Galvanic replacement reaction was used to prepare dendritic Ag/Cu. It showed that Ag/Cu possessed high electrocatalytic activity toward BCBA electroreduction reaction. Based on the in situ FTIR data, the electroreductive dehalogenation process of BCBA on Ag/Cu was obtained and was regarded as a sequence of halide expulsions and hydrogen additions. Because the BDE value of C-Br bond was less than that of C-Cl bond, C-Br bond was prior to break. The main intermediate of electroreductive dehalogenation reaction of BCBA on dendritic Ag/Cu was 2-chlorobenzoate and the end product was benzoate. Theoretical calculation could complement and verify the result of experiment, and make the experiment result more precise.

References

1. Z. Ronen and A. Abeliovich, *Appl. Environ. Microbiol.*, 66 (2000) 2372.
2. K. Anandarajah, P.M. Kiefer, B.S. Donohoe and S.D. Copley, *Biochemistry*, 39 (2000) 5303.
3. B. Yang, G. Yu and X.T. Liu, *Electrochim. Acta*, 52 (2006) 1075.
4. C.A. Ma, M.C. Li, Y.N. Liu and Y.H. Xu, *Electrochim. Acta*, 55 (2010) 3171.
5. A. Habekost and N. Aristov, *Chemosphere*, 88 (2012) 1283.
6. Y. Xu and W.X. Zhang, *Ind. Eng. Chem. Res.*, 39 (2000) 2238.
7. C. Lettmann, K. Hildenbrand, H. Kisch, W. Macyk and W.F. Maier, *Appl. Catal. B: Environ.*, 32 (2001) 215.
8. K. Miyoshi, Y. Kamegaya and M. Matsumura, *Chemosphere*, 56 (2004) 187.
9. S.B. Rondinini, P.R. Mussini, F. Crippa and G. Sello, *Electrochem. Commun.*, 2 (2000) 491.
10. S. Rondinini, P.R. Mussini, P. Muttini and G. Sello, *Electrochim. Acta*, 46 (2001) 3245.
11. A. Gutés, C. Carraro and R. Maboudian, *J. Am. Chem. Soc.*, 132 (2010) 1476.
12. J.X. Fang, H.J.You, P. Kong, Y. Yi, X.P. Song and B.J. Ding, *Cryst. Growth Des.*, 7 (2007) 864.
13. X. Chen, C.H. Cui, Z. Guo, J.H. Liu, X.J. Huang and S.H. Yu, *Small*, 7 (2011) 858.
14. W. Zhang, F.T. Tan, W. Wang, X.L. Qiu, X.L. Qiao and J.G. Chen, *J. Hazard. Mater.*, 217-218 (2012) 36.
15. C.D. Gu and T.Y. Zhang, *Langmuir*, 24 (2008) 12010.
16. L. Wang, H.L. Li, J.Q. Tian and X.P. Sun, *ACS Appl. Mater. Interfaces*, 2 (2010) 2987.
17. M.H. Rashid and T.K. Mandal, *J. Phys. Chem. C*, 111 (2007) 16750.
18. X. Wen, Y.T. Xie, W.C. Mak, K.Y. Cheung, X.Y. Li, R. Renneberg and S. Yang, *Langmuir*, 22 (2006) 4836.
19. A.A. Isse, B. Huang, C. Durante and A. Gennaro, *Appl. Catal. B: Gen.*, 126 (2012) 347.
20. C. Durante, B. Huang, A.A. Isse and A. Gennaro, *Appl. Catal. A: Gen.*, 126 (2012) 355.
21. C. Durante, V. Perazzolo, L. Perini, M. Favaro and G. Granozzi, A. Gennaro, *Appl. Cataly. B: Environ.*, 158-159 (2014) 286.
22. W.Z. Tang and C.P. Huang, *Waste Manage.*, 15 (1995) 615.
23. W.H. Wu, J. Xu and R. Ohnishi, *Appl. Cataly. B: Environ.*, 60 (2005) 129.
24. S.G. Sun, D.F. Yang and Z.W. Tian, *J. Electroanal. Chem.*, 289 (1990) 177.

25. R. Walsh, *Acc. Chem. Res.*, 14 (1981) 246.
26. R. Chetty, P.A. Christensen, B.T. Golding and K. Scott, *Appl. Catal. A: Gen.*, 271 (2004) 185.
27. R.D. Webster, *Electrochem. Commun.*, 5 (2003) 6.
28. N. Kumar, S. Thomas, R.B. Tokas and R.J. Kshirsagar, *Spectrochim. Acta A*, 118 (2014) 614.
29. H.Q. Li, S.G. Roscoe, J. Lipkowski, *J. Electroanal. Chem.*, 478 (1999) 67.
30. J. M. Delgado, A. Berná, J. M. Orts, A. Rodes, J. M. Feliu, *J. Phys. Chem. C*, 111 (2007) 9943.
31. M.C. Li, D.D. Bao, C.A. Ma, *Electrochim. Acta*, 56 (2011) 4100.
32. Y. Ikezawa, A. Yoshida, R. Sekiguchi, *Electrochim. Acta*, 2001, 46 (5) 769.
33. R. Chetty, P.A. Christensen, B.T. Golding, *Chemical. Commun.*, (2003) 984.
34. J. Suegara, B.D. Lee, M.P. Espino, S. Nakai, M. Hosomi, *Chemosphere*, 61 (2005) 341.